ORIGINAL ARTICLE

Pathologic Features of Tumor Activity and Stability in Uveal Melanoma Specimens after Fractionated CyberKnife Radiosurgery

Annette Zimpfer[1] · Bjoern Schneider[1] · Oliver Blanck[2,3] · Katrin Riedel[4] · Andrey Zhivov[5] · Danny Jonigk[6] · Andreas Erbersdobler[1] · Anselm Jünemann[4] · Nicolaus Andratschke[7,8] · Guido Hildebrandt[8] · Rudolf F. Guthoff[4] · Vinodh Kakkassery[4,9]

Abstract

To evaluate uveal melanoma cell activity and pathologic features after stereotactic CyberKnife radiosurgery in specimens from five patients. Specimens from five patients treated by CyberKnife radiosurgery in three fractions were included in this study. Because of persistent retinal detachment in 3 patients, tumour endoresection was performed at four, seven and ten month after CyberKnife radiosurgery. At nine and twelve months after treatment, enucleation of the eye globe was performed in 2 patients because of secondary tumour bleeding and missing regression. After histomorphological analysis and determination of Ki67-proliferation index, DNA cytophotometry, fluorescence in-situ hybridization evaluation for chromosome 3 loss, *GNA11* and *GNAQ* mutation analysis were performed. Four of the five tumours included in this study showed variable radiation-induced morphologic changes in the form of enlargement of cells and nuclei, cytoplasmic vacuolisation and nuclear fragmentation. The DNA content of a large fraction of tumour cells was hypoploid. On the other hand, single strikingly hyperchromatic melanoma cells showed marked aneuploidy. The proliferation fraction in the three endoresected tumours was very low (<1%), but it was elevated in the enucleation cases. Monosomy 3 was detected in two of the endoresection cases, but none of the enucleation cases. None of the patients experienced a local tumour recurrence, but two of the patients developed liver metastasis. Many melanoma cells seemed to be vital within the first 6 months after CyberKnife radiosurgery, but obvious radiation-induced morphologic changes, including tumour necrosis, hypoploid DNA content plus low Ki-67 index could indicate sublethal cell damage.

Keywords Uveal melanoma · CyberKnife · Stereotactic radiosurgery · Proliferation index · DNA image cytometry

✉ Annette Zimpfer
annette.zimpfer@med.uni-rostock.de

Bjoern Schneider
bjoern.schneider@med.uni-rostock.de

Oliver Blanck
oliver.blanck@uksh.de

Katrin Riedel
katrin.riedel@med.uni-rostock.de

Andrey Zhivov
a.zhivov@osg.de

Danny Jonigk
jonigk.danny@mh-hannover.de

Andreas Erbersdobler
andreas.erbersdobler@med.uni-rostock.de

Anselm Jünemann
anselm.juenemann@med.uni-rostock.de

Nicolaus Andratschke
nicolaus.andratschke@usz.ch

Guido Hildebrandt
guido.hildebrandt@uni-rostock.de

Rudolf F. Guthoff
rudolf.guthoff@med.uni-rostock.de

Vinodh Kakkassery
vinodh.kakkassery@uni-luebeck.de

Extended author information available on the last page of the article

Introduction

Uveal melanoma (UM) is the most common primary intraocular malignancy in adults [1, 2]. The incidence of this malignancy in the Caucasian population is 2 to 8 cases per million individuals per year [3–5]. Further, 50% of patients show an aggressive disease course and develop metastases [6].

Several therapeutic options are available for the treatment of UM, including resection or enucleation and eye globe-sparing modalities such as brachytherapy and teletherapy with proton beam [6–8]. Small tumours are generally treated with radioactive plaque brachytherapy with iodine-125, and ruthenium-106 or palladium-103, which is the primary treatment method of choice. However, with this method, the treatment depth is not reliable for large UM. When ruthenium plaques are used, optimal treatment responses are attained in tumors with diameter in the range of 8–10 mm [7–9]. Recent advances have led to the establishment of a new stereotactic radiosurgery approach in the form of the GammaKnife (Elekta AB, Sweden), CyberKnife (CK) (Accuracy Inc., U.S.A.) or linear accelerator-based radiosurgery systems [10–13].

Previous reports show good tumour control and low recurrence rates after brachytherapy [14–17]. According Damato and colleagues the rates of tumour recurrence following brachytherapy were 1%, 2%, and 3% at 2, 5, and 7 years, respectively [14]. Also, brachytherapy combined with transpupillary thermotherapy leads to excellent tumour control with 3% recurrences after 5 years [17]. There have been reports on the histopathologic changes in enucleated eyes after brachytherapy in UM [18–22]. Histopathologic examinations of UM specimen after brachytherapy revealed higher degrees of necrosis, balloon cell degeneration, inflammation, vascular damage and fibrosis in irradiated UM than in non-irradiated UM cases [19, 21]. Radiation therapy previous to enucleation significantly reduced numbers of mitotic figs. [18, 20–22]. The histopathological tumor cell activity features after stereotactic CK radiosurgery to treat uveal melanoma are rarely described. The objective of this study was to evaluate uveal melanoma cell activity by morphological analysis, immunohistochemistry and DNA cytophotometry after stereotactic CK radiosurgery in specimens from five patients.

Material and Methods

Patients and Treatment Modalities

The study was performed according to the tenets of the Declaration of Helsinki, and was approved by the university institutional review board (No. A2015–0171). All the subjects provided their written informed consent for participation.

Cybernknife Radiosurgery Modalities

For CK radiosurgery, complete immobilization of the eyeball was achieved by induction of retrobulbar anesthesia for each fraction, and planning imaging, treatment planning and treatment itself were performed in less than 3 h, the duration the anesthesia is effective. In the five patients, who underwent CK radiosurgery, a total dose of 60 Gy was delivered in three or four fractions in patients 1–4, and a total dose of 45 Gy was delivered in three fractions in patient 5 (Table 1).

Decision Rational for Endoresection or Enucleation after Cyberknife Radiosurgery

After CK radiosurgery, an ophthalmologic examination including funduscopy and B-wave-ultrasonography was performed in each patient every 3 month. Because of persistent tumour induced retinal detachment in 3 patients, endoresection was performed between four and seven months after the CK procedure. Further, tumour bleeding and missing regression was observed in 2 patients after 8 months and after 13 month, leading to the decision to enucleate the eyes (Table 1). For patient 1–5, the primary mean apical tumour height was 7.4 ± 2.9 mm.

Specimen Processing

In patients 1–3, about 300 ml of bloody cell solutions of the endoresected tumour specimens were sent immediately to the Institute of Pathology, University Pathology, University Medical Center Rostock. The fresh cell solutions were processed as follows: After centrifugation (2500 rpm, 10 min), 4 to 8 slides were prepared from the cell concentrates and stained with Papanicolaou, May-Grunwald-Giemsa, hematoxylin & eosin (H&E) and peroxidase-Schiff (PAS) according to standard protocols.

Because the samples had not been heparinized, cell clots were present in the fresh cell solutions. The cell clots were fixed in 4% formalin and embedded in paraffin to prepare cell blocks. The blocks were cut into 2-, 3- or 5-μm sections and mounted on charged slides for special staining, immunohistochemical analysis, fluorescence in-situ hybridization (FISH) and mutation analysis.

The enucleated eyeball specimens (cases 4 and 5) were processed as follows: After fixation in 4% formalin, the specimen was cut into serial sections (lateral to medial). After paraffin embedding, the tissue blocks were cut into 2- to 3-μm sections and stained with H&E and PAS. Then, these sections were mounted on charged slides and used for immunohistochemical staining. Additionally, 5-μm sections on charged slides were prepared for FISH. Enucleated tumours were classified according to the 8th edition of the Union for International Cancer Control / American Joint Committee on Cancer TNM classification and graded according a modified Callender classification [23, 24].

Table 1 Characteristics of five patients with choroidal melanoma who underwent CyberKnife radiosurgery

Patient no.	Age (y)	Sex	lt.	Apical tumor height (mm)	Dose	Follow-up sonography	Reason for endoresection/enucleation
1	47	m	l	9.7	2 × 12 Gy 2 × 18 Gy	Tumour height stable, reduction in vascularization	Persistent retinal detachment
2	66	f	r	9.6	3 × 20 Gy	Reduction in tumour height and vascularization	Persistent retinal detachment
3	68	f	r	7.0	3 × 20 Gy	Tumour height stable, slight reduction in vascularization	Persistent retinal detachment
4	70	m	r	7.99	3 × 20 Gy	Initial increase, followed by a reduction in tumour height, increase in vascularization at 6 months after CK radiosurgery	Tumour re-growth
5	57	m	l	3.17	3 × 15 Gy	Reduction of tumour height, new peripapillary tumor growth 11 months after CK radiosurgery	Tumour re-growth

f female, *lt* laterality, *l* left globe, *m* male, *r* right globe

Morphological Evaluation

To assess the extent of therapy-induced changes, the following morphological features were evaluated: nuclear changes such as nuclear swelling, nuclear vacuolisation, karyorrhexis, karyopyknosis, and formation of apoptotic bodies, and degenerative cytoplasmic changes such as cytoplasmic vacuolization, necrosis, inflammation, production of histiocytes, fibrosis, and vascular changes such as hyalinisation and occlusion.

Immunohistochemistry

Primary antibodies against Melan A (clone A103; DAKO Germany GmbH) (1:100, 20 min at 97 °C and pH 9), melanosome (clone HMB45; DAKO Germany GmbH) (1:50, 20 min at 97 °C and pH 9) and Ki67 (clone Mib-1; DAKO Germany GmbH) (1:500, 20 min at 97 °C and pH 9) were used. The standard immunoperoxidase technique was performed with an automated immunostainer (DAKO link) and diaminobenzidine as the chromogen. Melanoma or lymphatic tissues were used as the positive control.

DNA Ploidy Analysis

The DNA content was analyzed by image cytometry with a computer-aided image analysis system (AHRENS-ICM). The system measures the optical density on Feulgen-stained histological sections. Three-micrometer sections of the formalin-fixed/paraffin-embedded cell blocks (cases 1–3) or tissue blocks (specimens 4 and 5) were used.

Briefly, the slides were fixed in 4% buffered formalin, placed in 5 N HCl at room temperature for acid hydrolysis, stained in Feulgen solution for 1 h, and then rinsed thoroughly with water for 15 min. DNA cytophotometry was performed within 14 days after the slides were prepared.

The integrated optical density (IOD) of >400 tumour cells and > 30 reference cells (retinal cells and lymphocytes) was measured (wavelength, 570 nm). Digital images of the selected nuclei were converted into pixels and quantified with respect to the IOD, which integrates the DNA content and morphological features of the target nuclei, such as size, shape, contour, granularity, and chromatin texture as previously described [25]. The DNA histograms were interpreted as follows: hypodiploid cells ($n < 1.6c$), diploid cells ($n = 1.8$–$2.2c$), near diploid cells ($n > 2.2$–$2.4c$), mild aneuploidy ($n > 2.4$–$5c$), tetraploidy ($n = 4c$), and severe aneuploidy ($n > 5c$) (the criteria are modified from Schilling et al.'s criteria [26]).

Fluorescence-In-Situ Hybridization

Five-micrometer paraffin-embedded tissue/cell block sections were dewaxed with Roti-Histol (Roth, Karlsruhe, Germany) and incubated in an ethanol series (with decreasing concentrations) and finally in water. The FISH procedure was performed with the ZytoLight FISH tissue implementation kit (Zytomed Systems, Berlin, Germany) according to the manufacturer's recommendations. Probes for the centromere of chromosome 3 (CEN3; ZyOrange, Zytomed Systems) and chromosome 8 (CEN 8; ZyGreen, Zytomed Systems) were mixed at a ratio of 2:1, and 15–20 μl of the mixture was used for hybridization. After hybridization and washing, the slides were counterstained with DAPI/antifade solution (Zytomed Systems). At least 100 interphase tumour cell nuclei were counted. The cut-off limit for the deletion (monosomy 3) was >15%, and for chromosomal gain, it was 10% of the nuclei with three or more signals [27].

GNAQ and *GNA11* Mutation Analysis

DNA was extracted from FFPE sections by deparaffinization, proteinase K digestion and subsequent clean-up using Wizard DNA Clean-up System (Promega, Mannheim, Germany) according to standard protocols as previously reported [28]. The following genomic regions of interest were amplified by PCR: *GNAQ* exon 4 (forward primer: GCTTTGGTGTGATG GTGTCA, reverse primer: TCATGGACTCAGTTACTACC

TGA), *GNAQ* exon 5 (forward primer: TTTCCCTA AGTTTGTAAGTAGTGCT, reverse primer: CCATTCCC CACACCCTACTT), *GNA11* exons 4 (forward primer: TGCTGTGTCCCTGTCCTG, reverse primer: CACACCGG GCAAATGAGC), and *GNA11* exons 5 (forward primer: GATTGCAGATTGGGCCTTGG, reverse primer: CTTGGCAGGTGGGGAAGG). Twenty-five microliter of reaction mixtures contained 0.2 μl MyTaq polymerase with 5 μl 5x PCR buffer (Bioline, Luckenwalde, Germany), 1 μM of each primer set and 75 ng of template DNA. PCR reaction was carried out as follows: reactions were started at 95 °C for 1 min. This was followed by 35 cycles at 95 °C for 15 s, 58 °C (*GNAQ/GNA11*) for 15 s and 72 °C for 10s. As control, 10 μl of each PCR product were visualized on an agarose gel. PCR products were purified with alkaline phosphatase (Thermo Scientific, Darmstadt, Germany) and exonuclease I (Thermo Scientific). Subsequently, sequencing reaction was performed using BigDye Terminator v1.1 Cycle Sequencing Kit (Applied Biosystems, Darmstadt, Germany) with each pair of forward and reverse primers, followed by analysis on a 3500 genetic analyzer (Applied Biosystems). The sequence data were compared with reference sequences (*GNAQ*: ENSG00000156052, *GNA11*: ENSG00000088256) using SeqScape Software v2.7 (Applied Biosystems).

Statistical Analysis

Statistical analysis was performed using the Statistical Package of Social Sciences (Version 22.0, IBM, U.S.A.). Descriptive statistical tests were used to analyze continuous and categorical variables. Mean and standard deviation were calculated for continuous variables, and frequencies and relative frequencies were calculated for categorical variables.

Results

Clinicopathological Characteristics Prior to Endoresection or Enucleation

Patient data on tumour height, localization, CK treatment modalities and ultrasonographic follow-up are presented in Table 1. Doppler-coded ultrasound examination and fundus photography revealed a (slight) reduction in tumour vasculature in patients 1–3, and an increase in vascularisation in patient 4. CT scans showed regression of the apical tumour height in patients 1–3 (a reduction of 0.17 ± 0.55 mm) prior to tumour endoresection. Patient no. 2 was a 66-year-old female in whom liver metastases were diagnosed 6 months after CK treatment. In patient no. 4, follow-up sonography revealed missing tumour regression 6 months as well as bleeding after CK radiosurgery. Moreover, liver

metastases were found 11 months after CK treatment. In patient 5, a new peripapillary tumour was found 11 months after CK treatment.

Cyto/Histomorphological Assessment

In specimens 1–3, vital epitheloid melanoma cells or epitheloid and spindle cell type A and B were found, many of which displayed at least moderate degenerative features such as vacuolisation of the cytoplasma and karyoplasma (Fig. 1a–c). Many tumour cells in specimens 1–3 showed slight to moderate nuclear swelling and hypochromasia (Fig. 1a–c). Nuclear pyknosis and a few karyorrhectic figures and apoptotic bodies were observed in each specimen (Fig. 1c). Some fibrotic tissue fragments and a varying numbers of pigmented tumour cells as well as melanophages were observed in all three endoresected specimens (Fig. 1a–c). Also, hyaline vascular changes were seen in tiny edematous tumour fragments in specimens 1–3. In the smears, a background of necrotic debris and blood was observed (Fig. 1a–c). Vital melanoma cells of the epitheloid type were found in each case, but their number was considerably reduced in specimen 2 due to obviously extensive tumour necrosis (>50% tumour necrosis). In specimen 1 and 2, some lymphocytes were found, and in specimen 3, a relevant lymphohistiocytic inflammatory cell component was present. No mitotic figures were observed in one of the 3 endoresected specimens.

In specimen 4, a mushrooming head of an 8-mm tall pigmented choroidal tumour was found. The tumour had caused exsudative serous detachment of the overlying and adjacent retina (Fig. 1d). The Bruch membrane was intact. The detached retina showed photoreceptor atrophy and microcystic retinal degeneration. The melanoma was composed of vital epitheloid cells and type B spindle cells (Fig. 1e). The melanoma cells were admixed with several melanophages. No tumour necrosis was observed. An initial invasion of the sclera and venous invasion were demonstrated. Single mitotic figures were found in the H&E-stained sections. After routine histomorphological work-up the tumour was classified as UM with mixed cell type according modified Callender's classification and staged as T2a tumour.

In specimen 5, the choroidea showed focal fibrosis and thickened vascular channels with many melanophages and single bizarre epitheloid cells with striking cytopathic cell effects (Fig. 1f). Adjacent to the optic disc, a small tumour nodule of 2.5-mm height and predominant epitheloid cell morphological features was observed (Fig. 1f). Additionally, an initial scleral invasion, tumour invasion in an emissary canal and perineural invasion were found. Partial invasion of the optic nerve was seen, but no extrascleral extension of the
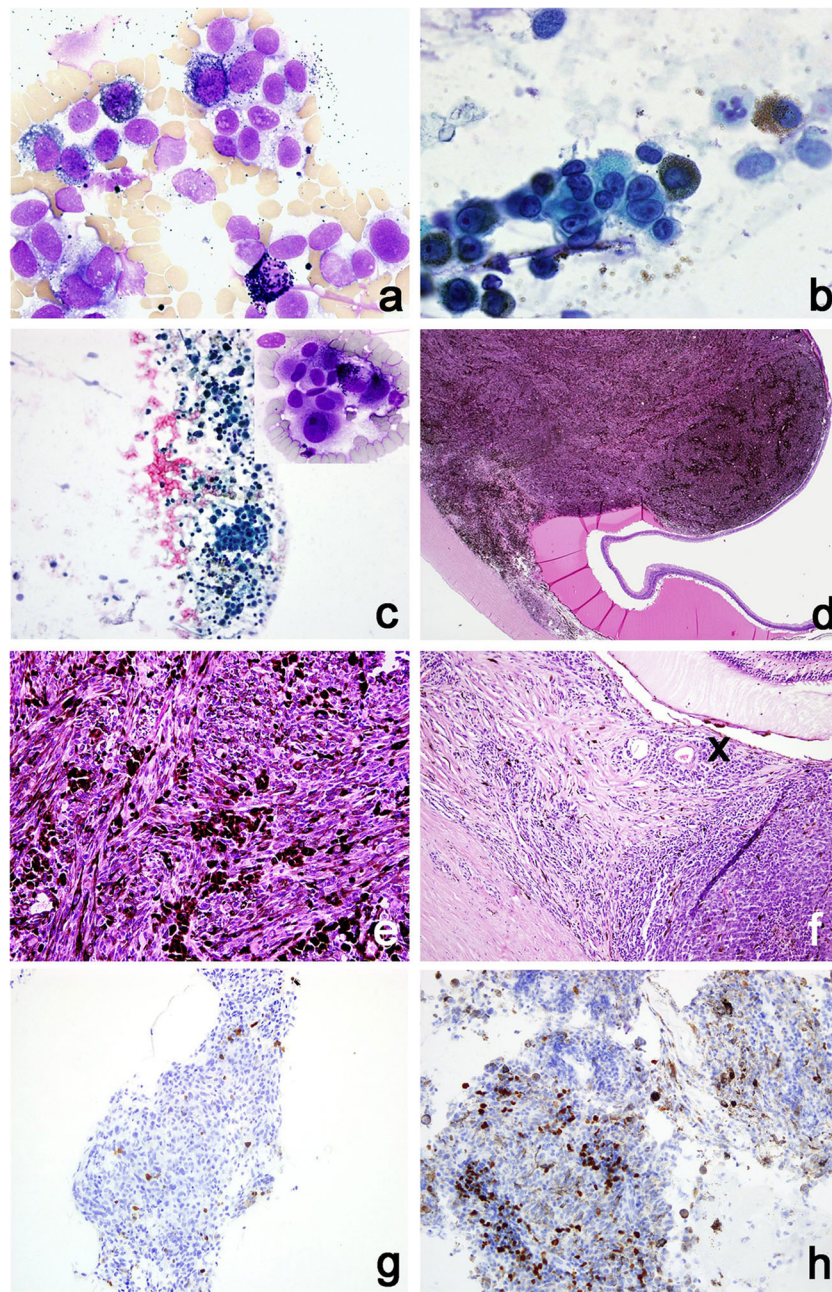
Fig. 1 Cytological and histological assessment of endoresected and enucleated specimens after CyberKnife radiosurgery. (**a**) Specimen 1: May-Grunwald-Giemsa (MGG)-stained smear displaying partially pigmented atypical epitheloid cells with degenerative features such as hypochromasia and vacuolisation of the cytoplasm. Note the bloody and necrotic background and the few pigment-laden macrophages (MGG, 100x). (**b**) Specimen 2: Papanicolaou-stained smear with vital, partially pigmented tumour cells and necrotic detritus in the background (Pap, 100x). (**c**) Specimen 3: Papanicolaou-stained smear with vital, partially pigmented epitheloid and spindle-shaped tumour cells and necrotic detritus and blood in the background (Pap, 20x). The inset shows vital epitheloid tumour cells and two karyorrhectic figures (MGG, 100x). (**d**) and (**e**) Specimen 4: A mushroom-shaped pigmented choroidal melanoma with exsudative serous detachment of the overlying and adjacent retina is seen. The partially heavily pigmented melanoma displays epitheloid and spindle cell type B tumour cells (H&E, 4x). (**f**) Specimen 5: The choroidea showed focal fibrosis and hyalinised vascular channels (x) with melanophages and single bizarre epitheloid cells with cytopathic effects. Beside this area, a small tumour nodule of predominant epitheloid cell morphology was seen. Additionally, an initial invasion of the sclera and emissary canal was demonstrated (H&E, 10x). (**g**) Specimen 2: The proliferation index was <1% in tumour cells (Ki67 immunohistochemistry, 10x). (**h**) Specimen 3: The proliferation index was <1% in melanoma cells, but elevated in the reactive lymphocytic infiltrate (Ki67, 10x)

tumour was observed. In all specimens, variable strong MelanA and melanosome immunoreactivity was observed (Fig. 1g). The tumor was classified as UM with mixed cell type and staged as T4a tumour according TNM classification.

Proliferation Index

The proliferation fraction in specimens 1–3 was <1% (Fig. 1h). In specimen 3 some reactive bystander lymphocytes showed Ki67 expression (about 2%). Ki67 index was slightly elevated in specimen 4 (2%) and moderately elevated in specimen 5 (10%).

DNA Ploidy Analysis

In all specimens, beside many cytomorphologically vital near diploid or slightly aneuploid tumour nuclei (2.30c–2.93c), many hypoploid tumour cells and often hypochromatic or apoptotic tumour nuclei or nuclear fragments were observed (<1.6c). This visualised extensive tumour cell degradation. Additionally, single highly aneuploid and hyperchromatic tumour cells were observed (5c–33.7c) (Fig. 2).

Fluorescence-In-Situ Hybridization Findings

In specimen 1 and 2 a prognostically relevant monosomy of chromosome 3 was detected (40%) (Fig. 3a and b). Due to strong melanin pigmentation and tumour necrosis in specimen 2, strong background fluorescence was present, which hampered the analysis. In specimen 4, the nuclear count was extremely difficult because of cellular overlap. In specimen 5, one to three red signals of chromosome 3, and three to five green signals of chromosome 8 were observed and indicate aneuploidy of the tumour cells. The results are listed in Table 2.

GNAQ and GNA11 Mutation Analysis

A GNA11 exon 5 (Q209L) mutation was detected in specimen 1, 4 and 5. In specimen 3 no GNA11 exon 4 or 5 or GNAQ exon 4 or 5 mutation was found (wild-type). Similarly in
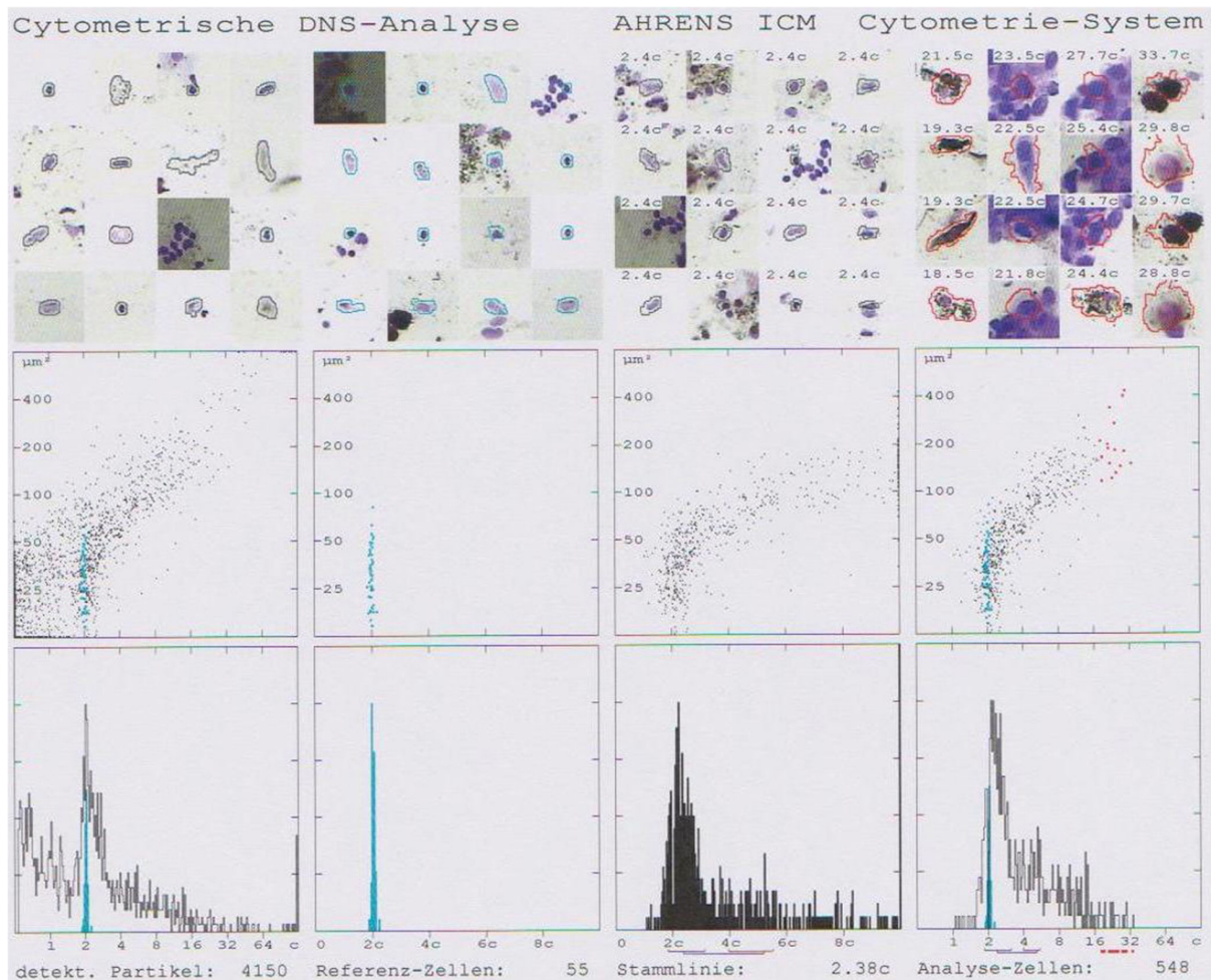

Fig. 2 DNA cytophotometry of a choroidal melanoma after CyberKnife radiotherapy. In case 4 the integrated optical density (IOD) of 548 tumour cells and 55 reference cells was measured (wavelength, 570 nm). The DNA histograms show a range of hypodiploid ($n < 1.6c$) to severe aneuploid tumour cells ($n > 5c$)
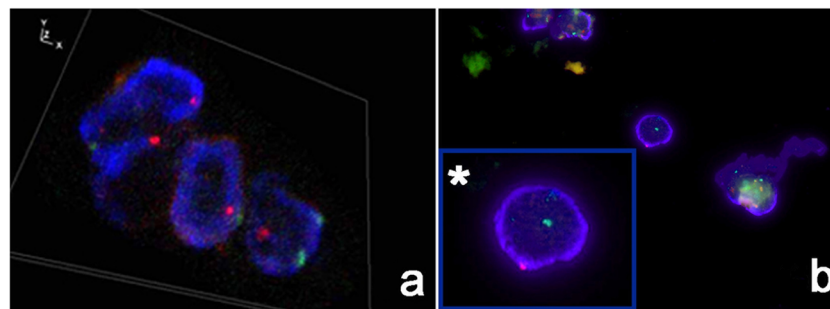
Fig. 3 Fluorescence-in-situ hybridization of chromosome 3 and 8. (**a**) and (**b**): Fluorescence-in-situ hybridization specimen 1 (**a**) and 2 (**b**) demonstrating monosomy of chromosome 3. Note: One red signal (chromosome 3) and two green signals (chromosome 8) were observed in two of three tumour cells in 3a and one tumour cell in 3b (enlarged in inset *)

specimen 2 wild-type situation was seen in *GNAQ* exon 4 and *GNA11* exon 5. The analysis of *GNAQ* exon 5 and *GNA11* exon 4 failed.

Discussion

GammaKnife radiosurgery was introduced in 1987 as a treatment option for eye melanomas [29]. The advantages are the possible preservation of the globe, the possible restoration of visual function and the availability of a non-invasive treatment option for large tumours [30].

There have been reports on the histopathologic changes in enucleated eyes after different forms of radiotherapy for uveal melanoma [18–22, 30–32]. However, the histopathological findings of the enucleated tissue after stereotactic CK or GammaKnife radiosurgery are rarely described. In one such study, Fernandes et al. demonstrated retinal damage and radiation-related retinal vascular changes such as fibrinoid necrosis and hyalinisation [33]. Further, Song et al. reported 50% - 100% tumour necrosis and the absence of mitotic activity in four of five tumours with persistent exsudative retinal detachment after CK radiosurgery [34].

The present study reports for the first time about CK radiosurgery induced cytomorphologic changes and aneuploidy

Table 2 Inter-phase FISH of chromosome 3 and 8 in irradiated choroidal melanoma tissue

Patient No.	Chromosome 3	Chromosome 8
1	Monosomy	Disomy
2	Monosomy	Disomy
3	Disomy	Disomy
4	Not evaluable	Not evaluable
5	Aneuploidy	Aneuploidy

Probes for the centromere of chromosome 3 (CEN 3; ZyOrange, Zytomed Systems) and chromosome 8 (CEN 8; ZyGreen, Zytomed Systems) were used

findings in uveal melanoma after tumour endoresection or enucleation. Gragoudas et al. evaluated the timeline of the histopathologic changes that occurred after treatment of uveal melanomas with proton beam therapy and enucleation [31]. The early effects were inflammation, which decreased with time. However, the incidence of fibrosis increased significantly with time, from 15% of the enucleation cases within 12 months (early cases) to >60% of the enucleation cases at more than 30 months (late cases) after irradiation. Moreover, tumour necrosis and blood vessel damage were observed early, and the prevalence of these changes was found to be constant over time. After exclusion of tumours with evidence of growth after irradiation, mitotic figures became progressively less common as the interval between irradiation and enucleation increased, and no mitotic figures were observed at more than 30 months after irradiation [31]. In the present study, the early findings were tumour necrosis and hemorrhage, which were observed in the endoresected specimens of patients 1–3; these findings are consistent with those of Gragoudas et al. The authors described necrotic changes in 50% of tumours that had been irradiated within the preceding year [31]. On the other hand, in patient 5, the extent of the widespread tumour necrosis could only be indirectly estimated owing to the extensive degenerative changes that occurred as a result of loss of tumour tissue, tissue edema, fibrosis and hyaline vascular changes, which occurred 12 months after irradiation and correspond to early irradiation effects described by Gragoudas and co-workers [31]. Heindl and colleagues also investigated the effects of brachytherapy on choroidal melanomas and showed that tumour necrosis, balloon cell degeneration, fibrosis and vascular changes corresponded significantly with the effects of the previous irradiation [19]. Similarly, Klaus and co-workers noted that fibrosis was only seen in the enucleated specimens after brachytherapy [18, 19]. In line with the study of Song et al., cytological changes, such as nuclear swelling, karyorrhexis, cytoplasmic vacuolization and hyaline vascular changes, which were observed in the endoresection specimens 1–3 and in specimen 5, could be interpreted as the cytomorphologic substrates of acute irradiation damage [34]. The described morphological

changes were observed in the interval of 6–12 months between CK radiosurgery and endoresection or enucleation pointing to a longer-lasting irradiation effect in the first months after CK radiosurgery.

Most uveal melanomas show a significant reduction in size after radiotherapy, but complete disappearance is not common [35]. Kang and colleagues reported the cumulative rate of tumour regression to be 18.8% in the first year and 42.8% in the second year after GammaKnife radiosurgery [30]. In the present study, the endoresection cases showed slight tumour regression, but the interval between irradiation and endoresection was only 6 months, which was too short to determine whether local tumour control could have been achieved or not [12].

The primary goals of radiotherapy in choroidal melanomas are ensuring local tumour control and preservation of the eye [11]. Regardless of local tumour control, some studies reported 4–18% metastasis 2–6 years after brachytherapy of uveal melanomas [19]. The underlying cause may have been chromosomal aberrations such as monosomy 3 and gains in chromosome 8q, which seem to directly affect the biological behavior of choroidal melanomas [27, 36–38]. In the present study, in two endoresection cases, prognostically significant monosomy 3 was detected. One of those two patients was diagnosed with liver metastasis 6 months after the initial diagnosis. Irrespective of the extent of tumour necrosis, especially in specimens 1–3, many tumour cells were preserved, as a result of which consecutive molecular studies could be conducted. FISH analysis of monosomy 3 was possible, as was Sanger sequencing for mutations in *GNAQ* and *GNA11* exon 4 and 5. In 60% of specimens a *GNA11* exon 5 mutation was detected, confirming driver mutation frequency in UM as previously shown [28].

In specimens 1–3 (no tumour re-growth), no mitotic figures were observed and the Ki67 index was <1%. Ki67 immunoreactivity in single cells was probably observed in reactive bystander lymphocytes. In specimens 4 and 5 (tumour re-growth) vital melanoma cells displayed a Ki67 index of 2% and 10%, respectively. In the literature, the significance of Ki67 frequency in irradiated melanomas is unclear. Biological tumour behavior in the presence of vital and proliferating tumour cells should be interpreted with caution. Chiquet and co-workers described a significant lower proliferation rate in choroidal melanomas after irradiation than in non-irradiated cases [39, 40]. The Ki67 score correlates with adverse prognostic parameters such as the mitotic index, largest tumour diameter, shrinking fibrosis and lack of obliterated vessels, and therefore the Ki67 score has a negative correlation with overall survival [40]. Using immunohistochemical proliferation markers in tumour cells treated with neoadjuvant therapy showed significantly lower proliferation activity than that in untreated tumours [18, 39–41]. However, according to Schilling, only a negligible Ki67-index (tumour cell proliferation) and the presence of

hypoploidy in DNA cytometry is a reliable indicator for irradiation-induced loss of proliferation potential [26].

Limitation of the present study are due to low number of cases and heterogeneity of specimens (enucleated or endoresected specimen). Furthermore, due to a short interval between CK radiosurgery and secondary endoresection/ enucleation only early irradiation effects in UM could be observed. Consecutively, early and late irradiation-associated changes in UM after CK radiosurgery should be analysed in a greater number of cases to gain insight in time-dependent tumour cell degradation, tumour shrinking and also irradiation side-effects in neighboring eye tissues.

In summary, many uveal melanoma cells seemed to be vital shortly after CK radiosurgery. Also, uveal melanoma cells displayed obvious radiation-induced morphologic changes after CK radiosurgery. Early irradiation effects in melanoma tissues are comparable to irradiation-induced changes after brachytherapy, protein beam radiation therapy and further irradiation therapies in UM.

Publisher's Note Springer Nature remains neutral with regard to jurisdictional claims in published maps and institutional affiliations.

References

1. Eagle CR (2011) Eye pathology. An atlas and text. Lippincott Williams & Wilkins, Philadelphia, pp 177–206

2. Font RL, Croxatto JO, Rao NA (2006) AFIP atlas of tumor pathology. Tumors of the eye and ocular adnexa. Armed Forces Institute of Pathology, Washington DC

3. Scotto J, Fraumeni JF, Lee JA (1976) Melanomas of the eye and other noncutaneous sites: epidemiologic aspects. J Natl Cancer Inst 56:489–491

4. Bergman L, Seregard S, Nilsson B, Lundell G, Ringborg U, Ragnarsson-Olding B (2002) Incidence of uveal melanoma in Sweden from 1960 to 1998. Invest Ophthalmol Vis Sci 43:2579–2583

5. Singh AD, Topham A (2003) Incidence of uveal melanoma in the United States: 1973–1997. Ophthalmology 110:956–961

6. Damato B (2012) Progress in the management of patients with uveal melanoma. The 2012 Ashton lecture. Eye (Lond) 2012 Sep; 26(9):1157-72. https://doi.org/10.1038/eye.2012.126

7. American Brachytherapy Society - Ophthalmic Oncology Task Force (2014) The American brachytherapy society consensus guidelines for plaque brachytherapy of uveal melanoma and retinoblastoma. Brachytherapy 13:1–14. https://doi.org/10.1016/j.brachy.2013.11.008

8. Damato B (1997) Adjunctive plaque radiotherapy after local resection of uveal melanoma. Front Radiat Ther Oncol 30:123–132

9. Bechrakis NE, Bornfeld N, Zoller I, Foerster MH (2002) Iodine 125 plaque brachytherapy versus transscleral tumor resection in the treatment of large uveal melanomas. Ophthalmology 109:1855–1861

10. Zorlu F, Selek U, Kiratli H (2009) Initial results of fractionated CyberKnife radiosurgery for uveal melanoma. J Neuro-Oncol 94: 111–117. https://doi.org/10.1007/s11060-009-9811-x

11. Wackernagel W, Holl E, Tarmann L, Mayer C, Avian A, Schneider M, Kapp KS, Langmann G (2014) Local tumour control and

gamma-knife radiosurgery of choroidal melanomas. Br J Ophthalmol 98:218–223. https://doi.org/10.1136/bjophthalmol-2013-304031

12. Schirmer CM, Chan M, Mignano J, Duker J, Melhus CS, Williams LB, Wu JK, Yao KC (2009) Dose de-escalation with gamma knife radiosurgery in the treatment of choroidal melanoma. Int J Radiat Oncol Biol Phys 75:170–176. https://doi.org/10.1016/j.ijrobp.2008.10.077

13. Sarici AM, Pazarli H (2013) Gamma-knife-based stereotactic radiosurgery for medium- and large-sized posterior uveal melanoma. Graefes Arch Clin Exp Ophthalmol 251:285–294. https://doi.org/10.1007/s00417-012-2144-z

14. Damato B, Patel I, Campbell IR, Mayles HM, Errington RD (2005) Local tumor control after (106)Ru brachytherapy of choroidal melanoma. Int J Radiat Oncol Biol Phys 63:385–391

15. Russo A, Laguardia M, Damato B (2012) Eccentric ruthenium plaque radiotherapy of posterior choroidal melanoma. Graefes Arch Clin Exp Ophthalmol 250(10):1533–1540. https://doi.org/10.1007/s00417-012-1962-3

16. Stoffelns BM, Kutzner J, Jochem T (2002) Retrospective analysis of ruthenium-106 brachytherapy for small and medium-sized malignant melanoma of the posterior choroid. Klin Monatsbl Augenheilkd 219(4):216–220. https://doi.org/10.1055/s-2002-30654

17. Shields CL, Cater J, Shields JA, Chao A, Krema H, Materin M, Brady LW (2002) Combined plaque radiotherapy and transpupillary thermotherapy for choroidal melanoma: tumor control and treatment complications in 270 consecutive patients. Arch Ophthalmol 120:933–940

18. Klaus H, Lommatzsch PK, Fuchs U (1991) Histopathology studies in human malignant melanomas of the choroid after unsuccessful treatment with106Ru/106Rh ophthalmic applicators. Graefes Arch Clin Exp Ophthalmol 229:480–486

19. Heindl LM, Lotter M, Strnad V, Sauer R, Naumann GO, Knorr HL (2007) High-dose 106Ruthenium plaque brachytherapy for posterior uveal melanoma. A clinico-pathologic study. Ophthalmologe 104:149–157. https://doi.org/10.1007/s00347-006-1451-3

20. no authors listed (1998) Histopathologic characteristics of uveal melanomas in eyes enucleated from the collaborative ocular melanoma study. COMS report no. 6. Am J Ophthalmol 125:745–766

21. Avery RB, Diener-West M, Reynolds SM, Grossniklaus HE, Green WR, Albert DM (2008) Histopathologic characteristics of choroidal melanoma in eyes enucleated after iodine 125 brachytherapy in the collaborative ocular melanoma study. Arch Ophthalmol 126:207–212. https://doi.org/10.1001/archopthalmol.2007.50

22. Shields CL, Shields JA, Karlsson U, Menduke H, Brady LW (1990) Enucleation after plaque radiotherapy for posterior uveal melanoma. Histopathologic findings. Ophthalmology 97:1665–1670

23. Brierley JD, Gospodarowicz MK, Wittekind C (eds) (2017) 8th edition of the Union for International Cancer Control / American Joint Committee on Cancer TNM classification. Wiley, Oxford

24. McLean IW, Foster WD, Zimmerman LE, Gamel JW (1983) Modifications of Callender's classification of uveal melanoma at the armed forces Institute of Pathology. Am J Ophthalmol 96:502–209

25. Gouvêa AF, Santos Silva AR, Speight PM, Hunter K, Carlos R, Vargas PA, de Almeida OP, Lopes MA (2013) High incidence of DNA ploidy abnormalities and increased Mcm2 expression may predict malignant change in oral proliferative verrucous leukoplakia. Histopathology 62:551–562. https://doi.org/10.1111/his.12036

26. Schilling H, Sehu KW, Lee WR (1997) A histologic study (including DNA quantification and Ki-67 labeling index) in uveal melanomas after brachytherapy with ruthenium plaques. Invest Ophthalmol Vis Sci 38:2081–2092

27. Van den Bosch T, van Beek JG, Vaarwater J, Verdijk RM, Naus NC, Paridaens D, de Klein A, Kiliç E (2012) Higher percentage of FISH-determined monosomy 3 and 8q amplification in uveal melanoma cells relate to poor patient prognosis. Invest Ophthalmol Vis Sci 53:2668–2674. https://doi.org/10.1167/iovs.11-8697

28. Schneider B, Riedel K, Zhivov A, Huehns M, Zettl H, Guthoff RF, Jünemann A, Erbersdobler A, Zimpfer A (2017) Frequent and Yet Unreported GNAQ and GNA11 Mutations are found in Uveal Melanomas. Pathol Oncol Res. https://doi.org/10.1007/s12253-017-0371-7

29. Rand RW, Khonsary A, Brown WJ, Winter J, Snow HD (1987) Leksell stereotactic radiosurgery in the treatment of eye melanoma. Neurol Res 9:142–146

30. Kang DW, Lee SC, Park YG, Chang JH (2012) Long-term results of gamma knife surgery for uveal melanomas. J Neurosurg 117:108–114

31. Crawford JB, Char DH (1987) Histopathology of uveal melanomas treated with charged particle radiation. Ophthalmol 94:639–643

32. Gragoudas ES, Egan KM, Saornil MA, Walsh SM, Albert DM, Seddon JM (1993) The time course of irradiation changes in proton beam-treated uveal melanomas. Ophthalmology 100:1555–1559

33. Singh AD, Eagle RC Jr, Shields CL, Shields JA (2003) Clinicopathologic reports, case reports, and small case series: enucleation following transpupillary thermotherapy of choroidal melanoma: clinicopathologic correlations. Arch Ophthalmol 121:397–400

34. Fernandes BF, Weisbrod D, Yücel YH, Follwell M, Krema H, Heydarian M, Xu W, Payne D, McGowan H, Simpson ER, Laperriere N, Sahgal A (2011) Neovascular glaucoma after stereotactic radiotherapy for juxtapapillary choroidal melanoma: histopathologic and dosimetric findings. Int J Radiat Oncol Biol Phys 80:377–384. https://doi.org/10.1016/j.ijrobp.2010.04.073

35. Song WK, Yang WI, Byeon SH, Koh HJ, Kwon OW, Lee SC (2010) Clinicopathologic report of uveal melanoma with persistent exudative retinal detachment after gamma knife radiosurgery. Ophthalmologica 224:16–21. https://doi.org/10.1159/000233231

36. Chappell MC, Char DH, Cole TB, Harbour JW, Mishra K, Weinberg VK, Phillips TL (2012) Uveal melanoma: molecular pattern, clinical features, and radiation response. Am J Ophthalmol 154:227–232. https://doi.org/10.1016/j.ajo.2012.02.022

37. Prescher G, Bornfeld N, Hirche H, Horsthemke B, Jöckel KH, Becher R (1996) Prognostic implications of monosomy 3 in uveal melanoma. Lancet 347:1222–1225

38. Coupland SE, Lake SL, Zeschnigk M, Damato BE (2013) Molecular pathology of uveal melanoma. Eye 27:230–242. https://doi.org/10.1038/eye.2012.255

39. Seregard S, Lundell G, Lax I, af Trampe E, Kock E (1997) Tumor cell proliferation after failed ruthenium plaque radiotherapy for posterior uveal melanoma. Acta Ophthalmol Scand 75:148–154

40. Chiquet C, Grange JD, Ayzac L, Chauvel P, Patricot LM, Devouassoux-Shisheboran M (2000) Effects of proton beam irradiation on uveal melanomas: a comparative study of Ki-67 expression in irradiated versus non-irradiated melanomas. Br J Ophthalmol 84:98–102

41. Pe'er J, Stefani FH, Seregard S, Kivela T, Lommatzsch P, Prause JU, Sobottka B, Damato B, Chowers I (2001) Cell proliferation activity in posterior uveal melanoma after Ru-106 brachytherapy: an EORTC ocular oncology group study. Br J Ophthalmol 85:1208–1212

Affiliations

Annette Zimpfer[1] (iD) · Bjoern Schneider[1] · Oliver Blanck[2,3] · Katrin Riedel[4] · Andrey Zhivov[5] · Danny Jonigk[6] ·
Andreas Erbersdobler[1] · Anselm Jünemann[4] · Nicolaus Andratschke[7,8] · Guido Hildebrandt[8] · Rudolf F. Guthoff[4] ·
Vinodh Kakkassery[4,9]

[1] Institute of Pathology, University Medical Center Rostock, Strempelstr. 14, 18057 Rostock, Germany

[2] Department for Radiation Oncology, University Medical Center Schleswig-Holstein, Arnold-Heller-Str. 3, 24105 Kiel, Germany

[3] Saphir Radiosurgery Center Northern Germany, Friedrich-Trendelenburg-Allee 2, 18273 Güstrow, Germany

[4] Department of Ophthalmology, University Medical Center Rostock, Doberaner Str. 140, 18057 Rostock, Germany

[5] OSG MVZ Betriebs GmbH, Ophthalmology, OMS, Anesthetics, Buger Str, 82 96049 Bamberg, Germany

[6] Hannover Medical School, Institute of Pathology, Carl-Neuberg-Str. 1, 30625 Hannover, Germany

[7] Department of Radiation Oncology, University Hospital Zurich, Rämistr. 100, 8091 Zurich, Switzerland

[8] Department of Radiotherapy, University Medical Center Rostock, Südring 75, 18059 Rostock, Germany

[9] Department of Ophthalmology, University-Hospital Schleswig-Holstein, University of Luebeck, Luebeck, Germany